Ceramics International 48 (2022) 27631–27636

Contents lists available at ScienceDirect

Ceramics International

journal homepage: www.elsevier.com/locate/ceramint

Waste-derived glass as a precursor for inorganic polymers: From foams to photocatalytic destructors for dye removal

Akansha Mehta [a,*], Elena Colusso [b], Jozef Kraxner [a], Dusan Galusek [a,c], Enrico Bernardo [b]

[a] FunGlass – Centre for Functional and Surface Functionalized Glass, Alexander Dubček University of Trenčín, Študentská 2, 911 50, Trenčín, Slovakia
[b] Department of Industrial Engineering, University of Padova, Via Marzolo 9, Padova, 35131, Italy
[c] Joint Glass Centre of the IIC SAS, TnUAD, and FChFT STU, Študentská 2, 911 50, Trenčín, Slovakia

ARTICLE INFO

Keywords:
Alkali activation
Gelation
Sorbents
Zeolites
Dye removal

ABSTRACT

Synthetic alumino-silicate glasses may yield inorganic polymers, through activation with alkali hydroxide solutions. In this framework, we formulated a glass prepared by the melting of red mud from bauxite refinement, combined with coal combustion fly ash, discarded pharmaceutical glass and a minor addition of sodium carbonate. The activation with 6 M NaOH aqueous solution allowed for the manufacturing of highly porous foams, by gas generation at the early stages of gelation. These foams featured an extensive formation of zeolite at cell walls which, combined with the presence of magnetite formed upon cooling of the melt, favoured the application of the foams as sorbents for dye removal from contaminated water. The powders prepared by crushing the highly porous foams showed an excellent water purification ability documented by efficient removal of methylene blue used as a model contaminant. The specific iron oxide polymorph facilitated both magnetic recovery of dispersed powders and photocatalytic destruction of the dye under UV irradiation.

1. Introduction

Sustainable management of hazardous inorganic waste from various industrial operations relies on a delicate balance between stabilization costs and benefits [1]. Vitrification is generally recognized as a key strategy for the stabilization of pollutants in a highly chemically stable matrix, but it is capital and energy intensive. The obtainment of glassy wasteforms to be disposed in landfills is not typically justified for industrial waste, contrary to the nuclear waste, for which permanent immobilization of radioactive ions in the glass structure has an absolute priority over the cost and energy consumption.

Vitrification studies on industrial waste, starting from the 1960's, have been accompanied by 'valorization' efforts. Waste-derived glasses are thus not considered as a final product, but can be utilized as a feedstock for new glass-ceramic products, especially construction materials, in the form of foams (for thermal insulation) or dense tiles (for the replacement of natural stones, such as marble and granite) [1]. The main challenge is the generation of an additional revenue from the new products, as an adequate compensation for the cost of vitrification. Such compensations is hardly achieved, if the products do not possess an intrinsic value (expressed by excellent mechanical and/or functional properties) compared to products from conventional feedstock. In addition, the new product implies remarkable additional transformation costs [1].

When transformed into new construction materials, waste-derived glasses typically undergo a second thermal treatment which, despite several optimizations (e.g long nucleation and crystal growth treatments, on bulk glass pieces replaced by fast sinter-crystallization of waste glass powders [1]), may impair the sustainability. The perspective of a 'cold' transformation, typical for alkali-activated materials [2], is then undoubtedly attractive as the means of reduction of transformation costs.

The conversion of waste glasses into glass-ceramics may be simplified by the adoption of a reference chemical composition, such as that of famous 'Slagsitalls', from $CaO–Al_2O_3–SiO_2$ glasses. Such standardization is helpful, since the particular formulation leads to a specified phase assemblage, favouring mechanical properties and chemical durability of the final products [1,3]. Glasses in the same compositional range may be obtained from a mixture of different wastes. Variations in the chemical composition of one constituent may be compensated by modifying the relative balance of the others [1].

To be considered for cold transformation, waste-derived glasses, the contents of oxides (alkali oxides, CaO, Al_2O_3 and SiO_2) must differ from those in Slagsitalls, i.e. match those of 'reactive' synthetic alumino-

* Corresponding author.
E-mail address: akansha.akansha@tnuni.sk (A. Mehta).

https://doi.org/10.1016/j.ceramint.2022.06.059
Received 25 March 2022; Received in revised form 2 June 2022; Accepted 5 June 2022
Available online 7 June 2022

silicate glasses. These are prepared by melting the batches based mainly on feldspars and clays, and can be transformed by alkali activation into stable inorganic polymers with a zeolite-like, alkali alumino-silicate hydrate gel structure [4–6]. Previous investigations have already indicated the possibility to synthesize a 'reactive' alumino-silicate glass from a mixture of wastes, comprising red mud from bauxite refinement, coal combustion fly ash and the glass from dismantled pharmaceutical vials [7].

Similarly to 'reactive' glasses, alumino-silicate waste may be also alkali activated and transformed into stable inorganic polymers with a zeolite-like, alkali alumino-silicate hydrate gel structure [8]. However, the transportation of inorganic waste, especially if it contains hazardous pollutants, is complicated and restricted by national and regional regulations. On the contrary, inert vitrified materials may be transported easily. In addition, the formation of inorganic polymers by condensation reactions at nearly room temperature requires a preliminary dissolution step in the solutions comprising only alkali hydroxides, instead of synthetic alkali silicates and aluminates [4–7].

Due to the high iron content resulting from the use of the red mud, the batch mentioned above did not yield homogeneous glass, and magnetite crystals (Fe_3O_4) separated upon cooling of the melt. Despite these inhomogeneities, almost no leaching of heavy metals from the waste-derived material was observed. After activation with 8 M NaOH aqueous solution a fine glass powder sieved below 75 μm formed a gel, eventually yielding a chemically stable cementitious material [7]. Although comparing well with 'lightweight concrete' (in terms density of 1.75 g/cm^3, bending strength of ~8 MPa, compressive strength of ~12 MPa), this material could not be considered as a final product. The magnetic functionality or the development of zeolite crystals in the gel were not fully exploited.

The present investigation offers a different perspective, yielding a product useable on multiple levels. First, the activating solution was modified to favour both zeolite formation and development of highly porous bodies by direct foaming of waste glass suspensions at an early stage of gelation. Second, powders from the crushing of foams were reused, suspended in methylene blue aqueous solutions, and tested as sorbents for the specific organic dye, which was then subjected to photocatalytic degradation under UV irradiation. The magnetic functionality was utilized for separating the sorbent from water.

2. Experimental procedure

According to the procedure described in our previous paper [5], a waste-derived glass was prepared by melting a mixture of red mud (RM), coal combustion fly ash (FA), pharmaceutical boro-alumino-silicate glass (BSG), and sodium carbonate at the weight ratios RM1/FA/BSG/Na_2CO_3 = 18/58/13/11. The batch was melted in a platinum crucible placed in a superkanthal ($MoSi_2$) furnace for 2 h at 1500 °C. The melt was then quenched, by pouring on a cold steel plate. Chemical composition of the glass was determined by X-ray fluorescence (XRF, Table 1).

Table 1
Chemical composition of starting waste and of the waste-derived glass.

	Red mud (RM1)	Fly Ash (FA)	Pharmaceutical glass (BSG)	Waste-derived glass
SiO_2	5.2	49.4	72.0	45.2
Al_2O_3	15	22.7	7.0	19.5
Fe_2O_3	52.9	7.4	–	15.3
Na_2O	2.4	0.9	6.0	8.5
K_2O	0.6	1.4	2.0	2.3
CaO	11.7	8.9	1.0	4.0
MgO	0.6	2.0	–	1.4
B_2O_3	–	–	12.0	1.2
TiO_2	–	–	–	–
Others	5.1	6.1	–	4.1

After cooling, the glass was hand crushed and dry ball milled (Pulverisette 6, Fritsch GmbH, Idar-Oberstein, Germany), to obtain a fine powder (<75 μm). The powder was placed in cylindrical polystyrene containers, at the 70–30 wt solid-liquid ratio and activated in alkaline solutions (4–10 M NaOH) under continuous mechanical stirring (300 rpm) for 90 min. After alkali activation, the suspension of partially dissolved glass powder was cast in closed polystyrene cylindrical moulds and cured at 75 °C for 2 h.

To prepare foams, sodium perborate monohydrate (SPB, $NaBO_3{\cdot}H_2O$, 1 wt% related to the glass content; Sigma Aldrich) or sodium dodecyl sulfate (SDS, $CH_3(CH_2)_{11}SO_4Na$, 1 wt% related to the glass content; Sigma Aldrich) were added to selected mixtures of partially dissolved fine powders and vigorously stirred for 10 min. The suspensions were then levelled out, the containers were covered by a lid and cured for 7 days at 40 °C.

Selected samples were characterized by infrared spectroscopy (FTIR 2000, PerkinElmer, Waltham, MA, USA), X-ray powder diffraction (XRD; Bruker D8 Advance, Karlsruhe Germany-CuKα radiation 0.15418 nm), helium pycnometry (Micromeritics AccuPyc 1330, Norcross, GA), optical stereomicroscopy (Carl Zeiss Microscopy, New York, USA), scanning electron microscopy (FEI Quanta 200 ESEM, Eindhoven, The Netherlands), and field-emission scanning electron microscopy (FE-SEM, Zeiss Sigma HD) operating at 3 kV, using a secondary electron detector. The phase identification from X-ray diffraction patterns was performed using the HighScore Plus (v. 3.0.4, PANanalytical B.V, Almelo, The Netherlands) supported by the PDF4+ 2014 database. The specific surface area, the total pore volume, and the pore size of the samples were evaluated by N_2 physisorption at −196 °C (ASAP 2010, Micromeritics, Norcross GA, USA).

Foamed samples were cut into approximately 12 mm × 12 mm x 12 mm cubic blocks, which were subjected to a compression test, using an universal testing machine (Quasar 25, Galdabini S.p.a., Cardano al Campo, Italy), operating at a cross-head speed of 1 mm/min. Each data point is the average of five independent measurements.

Residues from the crushing of foams were hand milled, sieved below 75 μm, and tested as sorbents for methylene blue dye. The powders (50 mg) were introduced in beakers containing 10 mL of a dye solution (100 mg/L), under magnetic stirring, and left in dark for 60 min. The suspensions were then UV irradiated (Hg lamp, λ = 366 nm, power = 125 W, Helios Italquartz S.R.L., Milan, Italy). The kinetics and concentration change of dye were recorded after removing the powders from suspensions with the use of a permanent magnet. The residues were filtered through a cellulose filter (0.22 μm), and a change of the absorption maximum of methylene blue at 660 nm was quantified with the use of a UV–Vis spectrophotometer (Jasco V570 spectrophotometer). Additional tests were performed also at lower amounts of powder (10 mg, 30 mg).

3. Results and discussion

Previous alkali activation studies, with the use of a 8 M NaOH solution, had led to the formation of a gel containing zeolite phases, such as sodium aluminium silicate hydrate (zeolite Y, $Na_{1.84}Al_2Si_4O_{11.92}{\cdot}7H_2O$, PDF#38–0238) and calcium aluminium silicate hydrate (cowlesite, $CaAl_2Si_3O_{10}{\cdot}6H_2O$, PDF#46–1405) [7]. The formation of these phases was found to be influenced by the concentration of the activation solution, as illustrated in Fig. 1.

A 'heavier' activation (10 M NaOH) favoured formation of an amorphous gel, as documented by the lower signal-to-background ratio of the diffraction pattern, and the presence of two broader diffraction maxima at 2θ~15° and 2θ~25°. Diffraction lines attributed to magnetite (Fe_3O_4, PDF#82–1533) were also present. These diffraction maxima (along with the minor ones) indicate the replacement of the zeolites mentioned above with a Na-based zeolite with a higher Al/Si ratio ($1.08Na_2O{\cdot}Al_2O_3{\cdot}1.68SiO_2{\cdot}1.8H_2O$, PDF#31–1271). A 'lighter' activation (4 M NaOH) did not cause any marked change of the diffraction pattern, compared to the as-prepared starting material. The only

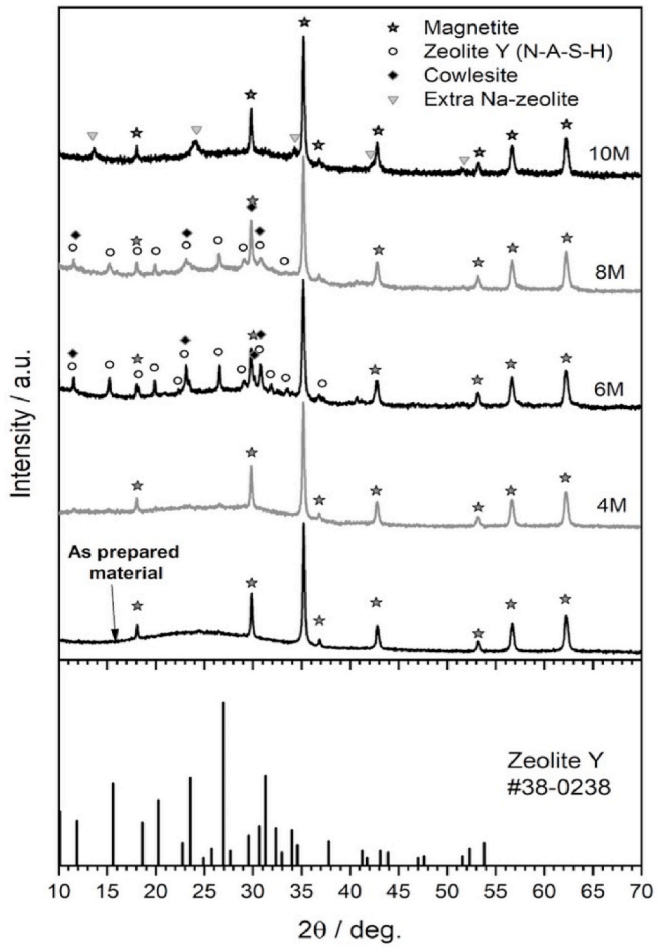

Fig. 1. Diffraction analysis of waste-derived alkali-activated materials.

difference was the shift of the hump centered at 2θ = 20–40° to higher 2θ values, characteristic for sodium alumino-silicate hydrated (N–A–S–H-type) gel [5]. The formation of zeolite Y was maximized after the activation with 6 M NaOH solution.

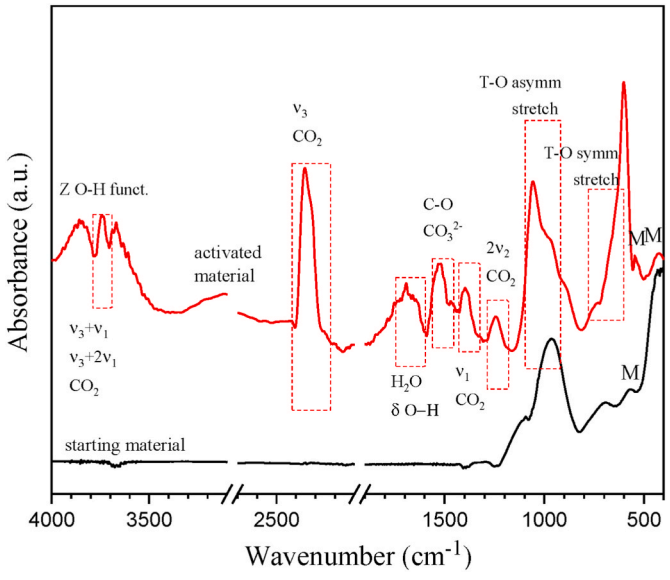

Fig. 2. FTIR spectra of the waste-derived material before and after activation (6 M NaOH).

Infrared spectroscopy study of the material activated with 6 M NaOH solution provided additional structural information (Fig. 2). The vibration modes between 900 cm^{-1} and 1200 cm^{-1} are assigned to asymmetric stretching vibrations of T-O bonds. Their positions are influenced by the amount of Al substituted in the tetrahedral (T) sites connected with the bridging oxygen atoms and the number of bridging vs. non-bridging oxygens. Deviation from a pure SiO_2 network leads to the observed shift to lower wavenumbers, as a result of the decreased bonding energy after the substitution [13]. The absorption at 650 cm^{-1} could be assigned to symmetric stretching vibrations of T-O bonds [7]. However, the origin of an intense peak centered at lower wawenumber; 470 cm^{-1} remain unclear. The absorption at low wavenumbers; 600 and 470 cm^{-1} may be attributed to the magnetite phase (marked by letter M in Fig. 2) [7]. The bands between 1600 cm^{-1} and 1500 cm^{-1} are related to the stretching vibration of carbonate groups, whereas the band at 1685 cm^{-1} is assigned to the stretching and bending vibrations of H–OH bonds. The peaks at 1400 and 1250 cm^{-1} could be attributed to CO_2 absorbed from the atmosphere, as previously observed for pure Na-zeolites [7].

Besides maximizing the formation of zeolite Y, uniform expansion was observed in the slurries activated by 6 M NaOH as a result of the addition of hydrated sodium perborate, as illustrated by the optical stereomicroscopy image in Fig. 3a. For its low cost and simplicity, the use of perborate was inspired by the preparation of highly porous geopolymers reported by Abdollahnejad at al [9]. Due to their characteristic low temperature decomposition, accompanied with the release of oxygen and water, perborates are widely used in the formulation of detergents and disinfectants, and in wood treatment [10]. The combination of the perborate with a surfactant tested in this study was based on a previous experience with the reduction of surface tension of geopolymer-yielding slurries, which prevented the coalescence of gas bubbles created as the result of addition of the foaming agent [11,12]. As pointed out by Budi [14], sodium perborate does not just dissolve in water, but interacts with it forming H_2O_2, ($NaBO_3+H_2O \rightarrow NaPO_2+H_2O_2$), which in alkaline environment decomposes, yielding water and oxygen.

Scanning electron microscopy revealed a 'hierarchical' porous structure. The cell walls were not compact, as it could be inferred from low magnification images (Fig. 3b), but were coated with numerous zeolite crystals (Fig. 3c), exhibiting a layer-like structure. Such structures are considered beneficial for the catalytic and adsorptive performance and are typically obtained from engineered formulations under optimized crystallization conditions [15].

As shown in Table 2, the foams were permeable, as documented by the almost completely open porosity. The abundant overall porosity (>80 vol%) and the characteristic nanoporosity of zeolites led to a high specific surface area of 83 m^2/g. The crushing strength was well below 1 MPa, but it should be noted that it remained close to the lower values exhibited by denser commercial cellular materials such as insulating concrete (compressive strength ranging from 0.5 to 8.2 MPa, with density ranging from 0.9 to 1.4 g/cm^3 vol%) [16]. Such highly porous foams may find additional use in various engineering applications, such as sound and thermal insulations [17].

A suggested application for the developed foams is the filtration of contaminated waters. This is supported by the reports on specific use of geopolymers and geopolymer-zeolite composites in dye removal [17,18]. The prepared foams can be used directly immersed in solutions [19]. However, this way the magnetism of the material cannot be exploited. This functionality offers an interesting 'end-of-life' option of powdered residues from mechanical testing, milled and sieved below 150 μm.

Granules prepared by sieving the powder (Fig. 3d) and still containing zeolite crystals formed during the activation were suspended in an aqueous solution of methylene blue and UV irradiated (Fig. 4).

Fig. 5a shows the absorbance spectrum of an aqueous solution of methylene blue (100 mg/L). The absorbance maximum at 660 nm was

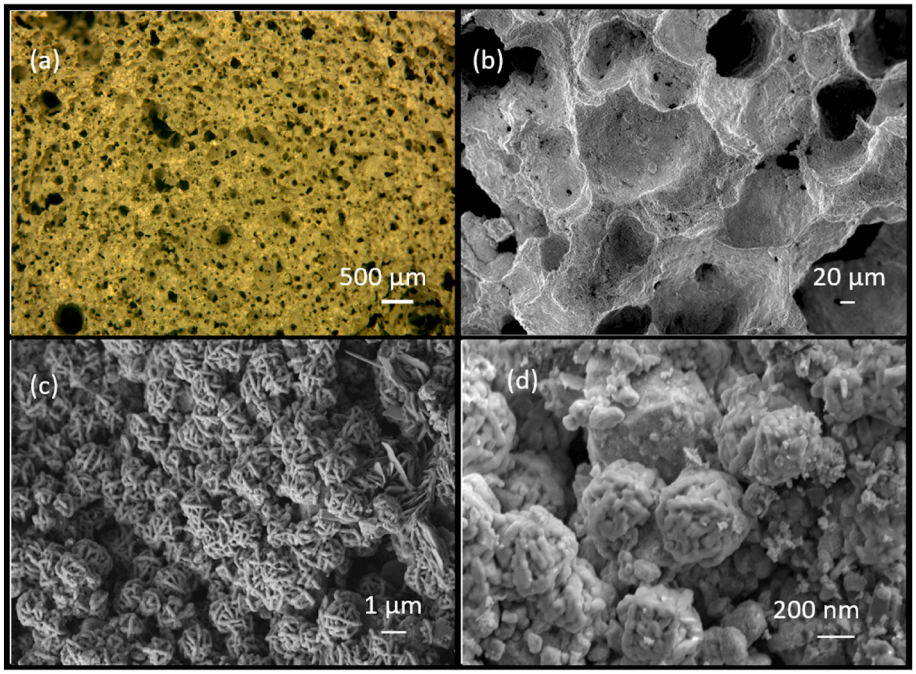

Fig. 3. Microstructure details of cellular body from direct foaming of suspension of waste-derived glass: a) low magnification stereomicroscopy image; b,c) scanning electron microscopy images at higher magnifications; d) after methylene blue degradation test. (For interpretation of the references to colour in this figure legend, the reader is referred to the Web version of this article.)

Table 2
Physical and mechanical properties of foams from alkali activation (6 M NaOH) of waste-derived glass.

Property	6 M NaOH activated foam
Density (g/cm^3)	0.42 ± 0.02
Total porosity (vol%)	82.1 ± 0.5
Open porosity (vol%)	81.5 ± 0.5
BET SSA (m^2/g)	83 ± 1
Crushing strength (MPa)	0.36 ± 0.04

considered as a reference for the initial concentration of the dye (C_0). The sensitivity to UV degradation of the specific organic species was documented by the decrease of absorbance after 30 min irradiation (a reduction of ~20% of the intensity of absorbance peak; $C/C_0 = 0.78$). The granules acted as an effective agent for dye removal even without UV irradiation. The granules were added to the solution. After 30 min exposure, the granules were magnetically separated: a significant reduction of methylene blue concentration was observed. In analogy with other alkali-activated materials, the methylene blue molecules were 'trapped' (adsorbed) by the granules.

In the following experiment, the adsorption and UV irradiation were combined: the absorbance spectrum of the methylene blue solution

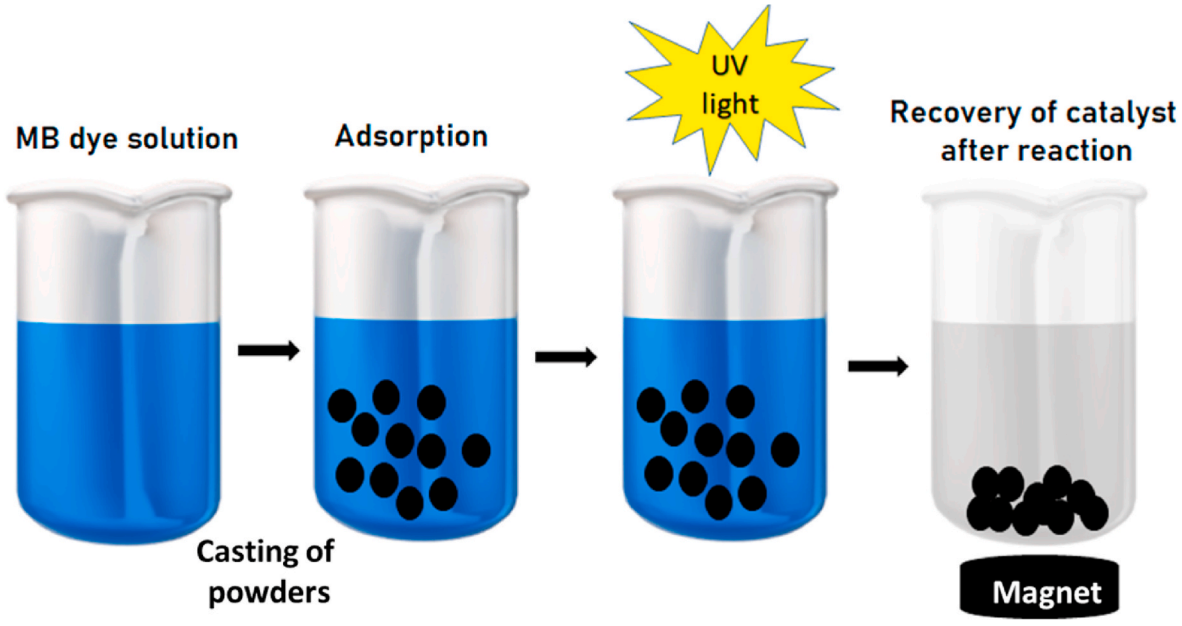

Fig. 4. Scheme of adsorption/irradiation and recovery.

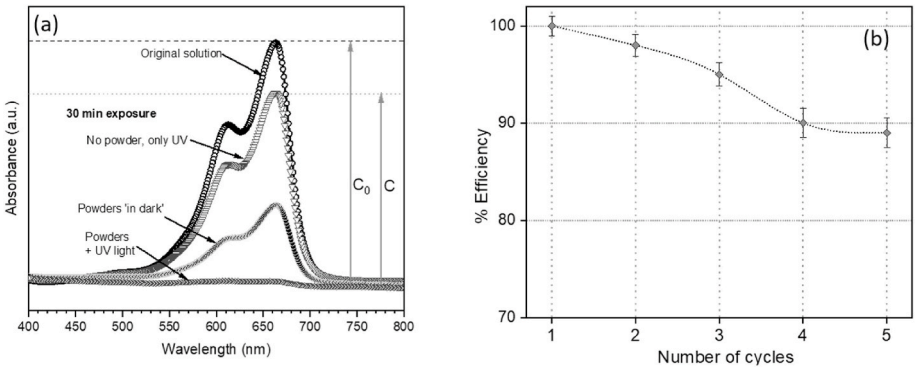

Fig. 5. a) Optical spectra reflecting the concentration of methylene blue in solution; b) Evolution of dye removal efficiency with the number of adsorption cycles.

containing suspended granules and exposed to UV irradiation revealed an almost complete removal of the dye. The dye removal could be also enhanced by the presence of magnetite, which is known to act as a photocatalyst in the specific field of dye degration [20].

The substantial dye removal efficiency was confirmed by repeating the adsorption/irradiation experiment for five times. After recovery, the activity of the powder remained almost completely preserved. Fig. 5b illustrates the change of 'efficiency' of dye removal, estimated by the equation:

$$Efficiency = \frac{C_o - C_{30\text{min}UV+powder,cycle\ n}}{C_o - C_{30\text{min}UV+powder,cycle\ 1}} \cdot 100\%$$

where C_o is the initial concentration of the dye solution and $C_{30\ \text{min}}$ is the concentration of dye solution after 30 min irradiation time. Nearly 90% of the initial performance was still preserved after 5 adsorption/recovery cycles.

Fig. 6 illustrates the relationship between the relative concentration of methylene blue solution and the exposition time under ultraviolet light. To evaluate the influence of the catalyst, different amounts of powder were mixed with the MB dye solution. The dye reduction rate increased with increasing concentration of the powder; the maximum extent of dye degradation efficiency >90% was achieved after 30 min of exposure if 50 mg of the powder was added. Only ~80% of the dye was removed with 10 mg powder addition. This indicates that the degradation is selective and depends on the amount of the catalyst. The increasing extent of degradation with 50 mg sample can be attributed to the increasing number of active surface sites which produce more radicals, accelerating the degradation rate.

The results of methylene blue degradation confirm the data from the literature [20–23]. The adopted waste-derived glass can be considered as a model for the preparation of components with complex functionalities. Future efforts will be dedicated to the exploration of new waste mixtures and new manufacturing technologies, including direct ink writing of pastes at early stages of gelation.

4. Conclusions

A waste-derived glass is an interesting precursor which, when activated by NaOH solutions, yields semi-crystalline inorganic gels, featuring Ca- and Na-based zeolites. The formation of zeolites is optimal after the activation in an alkaline solution of specified molarity (6 M NaOH). If small amounts of suitable additives (sodium perborate monohydrate or sodium dodecyl sulfate) are used, a substantial foaming of the activated suspensions of waste-derived glass is achieved. Powders prepared by crushing the foams act as efficient sorbents for the removal of organic dyes from water. The sorption and dye removal capacity of the powder remains almost unaffected even after five sorption/irradiation cycles. The magnetic functionality attributed to the presence of magnetite crystallizations from glass forming melt, allows for an easy separation of powders from the solution, with no need for centrifugation.

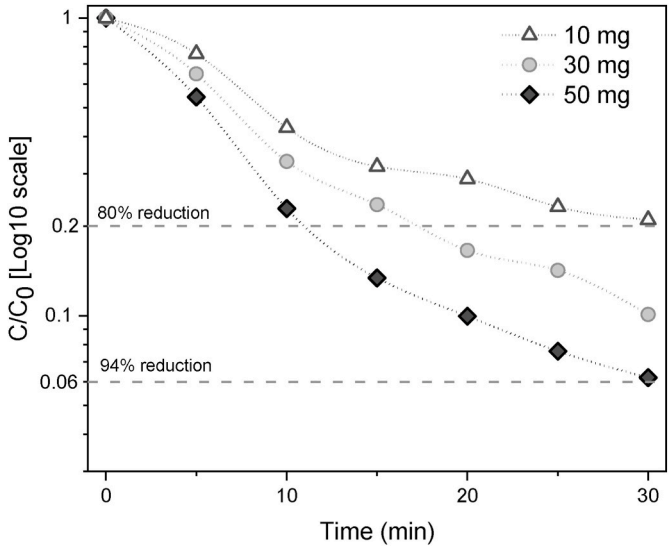

Fig. 6. Photocatalytic degradation of methylene blue solution under different catalytic conditions.

Declaration of competing interest

The authors declare that they have no known competing financial interests or personal relationships that could have appeared to influence the work reported in this paper.

Acknowledgements

This paper is a part of the dissemination activities of project "FunGlass" (Centre for Functional and Surface Functionalized Glass). This project has received funding from the European Union's Horizon 2020 research and innovation programme under grant agreement no. 739566. Enrico Bernardo acknowledges the additional funding from the University of Padova (Department of Industrial Engineering), in the framework of the "SusPIRe" (Sustainable porous ceramics from inorganic residues, BIRD202134). The authors thank Dr. Patricia Rabelo Monich (University of Padova, currently at Denmark Technical University) and Dr. Hamada Elsayed (University of Padova) for experimental assistance.

References

[1] A. Rincón, M. Marangoni, S. Cetin, E. Bernardo, Recycling of inorganic waste in monolithic and cellular glass-based materials for structural and functional applications, J. Chem. Technol. Biotechnol. 91 (2016) 1946–1961, https://doi.org/10.1002/jctb.4982.

[2] J.L. Provis, Geopolymers and other alkali-activated materials: why, how, and what? Mater. Struct. 47 (2014) 11–25, https://doi.org/10.1617/s11527-013-0211-5.

[3] E. Bernardo, L. Esposito, E. Rambaldi, A. Tucci, Y. Pontikes, G.N. Angelopoulos, Sintered esseneite–wollastonite–plagioclase glass–ceramics from vitrified waste, J. Eur. Ceram. Soc. 29 (2009) 2921–2927, https://doi.org/10.1016/j.jeurceramsoc.2009.05.017.

[4] I. Garcia-Lodeiro, A. Fernández-Jimenez, P. Pena, A. Palomo, Alkaline activation of synthetic aluminosilicate glass, Ceram. Int. 40 (2014) 5547–5558, https://doi.org/10.3389/fchem.2021.715052.

[5] I. Garcia-Lodeiro, E. Aparicio-Rebollo, A. Fernández-Jimenez, A. Palomo, Effect of calcium on the alkaline activation of aluminosilicate glass, Ceram. Int. 42 (2016) 7697–7707, https://doi.org/10.1016/j.ceramint.2016.01.184.

[6] C. Ruiz-Santaquiteria, A. Fernández-Jiménez, A. Palomo, Alternative prime materials for developing new cements: alkaline activation of alkali aluminosilicate glasses, Ceram. Int. 42 (2016) 9333–9340, https://doi.org/10.1016/j.ceramint.2016.03.111.

[7] M. Hujova, P.R. Monich, H. Kankova, H. Lucas, B. Xakalashe, B. Friedrich, J. Kraxner, D. Galusek, E. Bernardo, New glass-based binders from engineered mixtures of inorganic waste, Int. J. Appl. Glass Sci. 12 (2021) 570–580, https://doi.org/10.1111/ijag.16262.

[8] N. Toniolo, A. Rincón, Y.S. Avadhut, M. Hartmann, E. Bernardo, A.R. Boccaccini, Novel geopolymers incorporating red mud and waste glass cullet, Mater. Lett. 219 (2018) 152–154, https://doi.org/10.1016/j.matlet.2018.02.061.

[9] Z. Abdollahnejad, F. Pacheco-Torgal, T. Félix, W. Tahri, J.B. Aguiar, Mix design, properties and cost analysis of fly ash-based geopolymer foam, Construct. Build. Mater. 80 (2015) 18–30, https://doi.org/10.1016/j.conbuildmat.2015.01.063.

[10] E. Pesman, E. E Kalyoncu, H. Kirci, Sodium perborate usage instead of hydrogen peroxide for the reinforcement of oxygen delignification, Fibres Text. East. Eur. 18 (2010) 83.

[11] V. Phavongkham, S. Wattanasiriwech, T.W. Cheng, D. Wattanasiriwech, Effects of surfactant on thermo-mechanical behavior of geopolymer foam paste made with sodium perborate foaming agent, Construct. Build. Mater. 243 (2010), 118282, https://doi.org/10.1016/j.conbuildmat.2020.118282.

[12] L. Korat, V. Ducman, Characterization of fly ash alkali activated foams obtained using sodium perborate monohydrate as a foaming agent at room and elevated temperatures, Front. Mater. (2020) 308, https://doi.org/10.3389/fmats.2020.572347.

[13] X. Ke, S. A Bernal, N. Ye, J.L. Provis, J. Yang, One-part geopolymers based on thermally treated red mud/NaOH blends, J. Am. Ceram. Soc. 98 (2015) 5–11, https://doi.org/10.1111/jace.13231.

[14] A.T. Budi, The combination of sodium perborate and water as intracoronal teeth bleaching agent, Dent. J. 41 (2008) 186–189.

[15] B. Reiprich, T. Weissenberger, W. Schwieger, A. Inayat, Layer-like FAU-type zeolites: a comparative view on different preparation routes, Front. Chem. Sci. Eng. 14 (2020) 127–142, https://doi.org/10.1007/s11705-019-1883-3.

[16] CES (cambridge engineering selector) EduPack. https://www.ansys.com/it-it/products/materials/granta-edupack, 2020.

[17] P.S. Liu, G.F. Chen, Porous Materials: Processing and Applications, Elsevier, 2014.

[18] V. Medri, E. Papa, M. Mor, A. Vaccari, A.N. Murri, L. Piotte, C. Melandri, E. Landi, Mechanical strength and cationic dye adsorption ability of metakaolin-based geopolymer spheres, Appl. Clay Sci. 193 (2020), 105678, https://doi.org/10.1016/j.clay.2020.105678.

[19] K. Pimraksa, N. Setthaya, M. Thala, P. Chindaprasirt, M. Murayama, Geopolymer/Zeolite composite materials with adsorptive and photocatalytic properties for dye removal, PLoS One 15 (2020), https://doi.org/10.1371/journal.pone.0241603.

[20] D. Wattanasiriwech, K. Yomthong, S. Wattanasiriwech, Adsorption efficiency and photocatalytic activity of fly ash-based geopolymer foam mortar, Ceram. Int. 47 (2021) 27361–27371, https://doi.org/10.1016/j.ceramint.2021.06.158.

[21] T. de Oliveira Guidolin, N.M. Possolli, M.B. Polla, T.B. Wermuth, T.F. de Oliveira, S. Eller, O.R. Montedo, S. Arcaro, M.A. Cechinel, Photocatalytic pathway on the degradation of methylene blue from aqueous solutions using magnetite nanoparticles, J. Clean. Prod. 318 (2021), 128556, https://doi.org/10.1016/j.jclepro.2021.128556.

[22] L. Dashairya, A. Mehta, P. Saha, S. Basu, Visible-light-induced enhanced photocatalytic degradation of Rhodamine-B dye using $BixSb_2$-xS_3 solid-solution photocatalysts, J. Colloid Interface Sci. 561 (2020) 71–82, https://doi.org/10.1016/j.jcis.2019.11.118.

[23] P. Senthilkumar, D.A. Jency, T. Kavinkumar, D. Dhayanithi, S. Dhanuskodi, M. Umadevi, S. Manivannan, N.V. Giridharan, V. Thiagarajan, M. Sriramkumar, K. Jothivenkatachalam, Built-in electric field assisted photocatalytic dye degradation and photoelectrochemical water splitting of ferroelectric Ce doped $BaTiO_3$ nanoassemblies, ACS Sustain. Chem. Eng. 7 (2019) 12032–12043, https://doi.org/10.1021/acssuschemeng.9b00679.